

**Technical Note****Feasibility of Nonlinear Analysis for Seismic Design of RC Special Moment Frames****Sara Naghavi¹, Abdolreza S. Moghadam^{2*} and Mohammad Reza Mansoori³**

1. M.Sc. Graduate, Department of Civil Engineering, Science and Research Branch, Islamic Azad University, Tehran, Iran

2. Associate Professor, Structural Engineering Research Center, International Institute of Earthquake Engineering and Seismology (IIEES), Tehran, Iran,

*Corresponding Author; email: moghadam@iiees.ac.ir

3. Assistant Professor, Department of Civil Engineering, Science and Research Branch, Islamic Azad University, Tehran, Iran

Received: 31/01/2023

Revised: Not Required

Accepted: 15/03/2023

ABSTRACT**Keywords:**

Reinforced concrete special moment frames; Linear analysis; Nonlinear analysis; Optimal strength distribution pattern; Near-fault and far-fault ground motions

A performance-based procedure for the seismic design of reinforced concrete (RC) special moment frames is presented. The proposed method includes nonlinear static analysis in accordance with appendix 2 of BHRC and nonlinear dynamic analysis in accordance with chapter 16 of FEMA P-2082-1. The proposed method has been systematically applied to the design of a regular multistory 3-dimensional (3D) RC special moment frame then; its seismic performance has been compared with that of a similar frame designed according to BHRC under an ensemble of 22 near-fault and far-fault ground motions. The results show that the proposed method can better achieve the optimal strength distribution pattern over conventional method. Buildings designed with the proposed method showed better seismic performance than those designed according to the standard code. In addition, this method has been shown to be more economical than conventional design methods.

1. Introduction

While buildings are usually designed for seismic resistance using elastic analysis, most will experience significant inelastic deformations under large earthquakes. Modern performance based design (PBD) methods require techniques to determine the realistic behavior of structures under such conditions. Enabled by advancements in computing technologies and available test data, nonlinear analysis provides the means for calculating structural response beyond the elastic range, including strength and stiffness deterioration associated with inelastic material behavior and large displacements. As such, nonlinear analysis can play an important role in the design of new and existing buildings

(Carvalho et al., 2013; Deierlein et al., 2010; Fajfar, 2018; Rao et al., 2017; Li et al., 2019).

The initial seismic design of a regular structure in almost all current seismic design guidelines and codes of practice (e.g., ASCE/SEI 7-16; IBC; Eurocode; BHRC) is based on the equivalent static force method. This method determines the story shear strength and stiffness characteristics of the structural systems using design-spectrum compatible lateral force patterns. It is known that code-specified seismic design force patterns are based on the dynamic response of elastic structural systems and do not directly consider the inelastic behavior of the system. As such, these regulations

do not achieve a relationship between stability level, safety, cost and building performance against an earthquake (Ganjavi & Ghodrati Amiri, 2018; Park, 2005; Mergos, 2017). Researchers continue to look for methods that, in addition to time and cost effectiveness can accurately provide the main earthquake responses. One method for solving this problem is to use nonlinear analysis in the seismic design of buildings.

The first widespread practical applications of nonlinear analysis in earthquake engineering in the United States (US) were for assessment and retrofitting of existing buildings. The first significant guidelines on the application of nonlinear analysis were those published by Federal Emergency Management Agency (FEMA 273) and Applied Technology Council (ATC-40). Owing to the state of knowledge and computing technologies at the time of their publication (mid-1990s), these documents focus primarily on nonlinear static (pushover) analysis. They have since been carried forward into ASCE/SEI 41-06 and improvements have been proposed in FEMA 440, FEMA P440 and FEMA P-2082-1. While ASCE/SEI 41-06 and related documents primarily focus on renovating existing buildings, the nonlinear analysis, component modeling and acceptance criteria in these documents can be applied to new building designs, provided that the acceptance criteria address the performance levels required by ASCE/SEI 7-16 for new building design.

The role of nonlinear dynamic analysis for design is being expanded to quantify building performance more completely. ATC 58 employs nonlinear dynamic analysis for seismic performance assessment of new and existing buildings, including fragility models that relate structural demand parameters to explicit damage and loss metrics. Nonlinear dynamic analysis is also used to assess the performance of structural systems that do not conform to the prescriptive seismic force-resisting system types in ASCE/SEI 7-16.

Seismic design with nonlinear analysis enhances control over structural damage for different levels of earthquake hazard. Nevertheless, the number of studies dealing with this type of seismic design of reinforced concrete (RC) frames is limited. The initial studies on the seismic design of RC buildings

using nonlinear analysis were carried out by Fintel & Ghosh (1982), Kappos & Manafpour (2001) and Romao et al. (2002).

Fintel & Ghosh (1982) proposed an alternative standard code procedure for the seismic resistant design of structures. They selected earthquake accelerograms and used them for loading and dynamic inelastic response history analysis to determine the force on members and deformation. Their proposed method was applicable to steel and concrete buildings and has been used in RC buildings with coupled-walls and frame-walls.

Kappos & Manafpour (2001) presented a performance-based seismic design procedure for two distinct limit states using nonlinear dynamic (time-history) and static (pushover) analysis for the seismic design of 2D RC buildings. Their proposed method was found to lead to better seismic performance than the procedures in standard codes such as Eurocode, at least in the case of the regular multistory RC frame structures studied. In addition, it led to a more economical design.

Romao et al. (2002) presented a new seismic design that uses nonlinear dynamic analysis for the design of concrete buildings. This new method, along with Eurocode, was applied to a multi-story RC frame and the designs were evaluated using the estimation process for different criteria that provide different limit states.

Kappos & Panagopoulos (2004) studied the performance-based seismic design of 3D RC buildings using inelastic static and dynamic analysis. They presented a PBD procedure for realistic 3D RC buildings. They found that the proposed method leads to better seismic performance than the standard code procedure and results in a more economical design of transverse reinforcement in members that develop very little inelastic behavior, even in very strong earthquakes. This methodology was used in the US following several large earthquakes, particularly the 1994 Northridge earthquake, which caused major damage.

Kappos & Stefanidou (2010) proposed a new method for the seismic design of irregular concrete buildings using the method proposed by Kappos & Pungopoulos (2004). Their proposed method was applied to irregular multistory 3D RC frame buildings with setbacks to determine

their performance at several levels of earthquake action using a fully inelastic model and additional ground motions not used in the design phase. The same buildings were also designed according to the provisions of Eurocode. Comparison of the two methods revealed the advantages of the proposed design method. As in the previous method (Kappos & Panagopoulos (2004)), the proposed method led to more economical detailing of transverse reinforcement in members that develop very little inelastic behavior, even in very strong earthquakes. Gkatzogias & Kappos (2015) based on the method of Kappos & Stefanidou (2010) presented a rigorous design methodology for concrete bridges.

Teran-Gilmore et al. (2010) presented a numerical performance-based methodology for the predesign of reinforced concrete ductile structures.

Mergos (2018) proposed an iterative procedure for the design of reinforcement for RC frames using pushover and nonlinear response-history analysis in order to meet the performance objectives. He showed that the proposed procedure is more appropriate than existing methods.

Mergos (2020) employed nonlinear response-history analysis and pushover analysis with the N2 method in a computational framework for the minimum cost performance-based seismic design of reinforced concrete frames according to the fib Model Code 2010 methodology and compared their obtained design solutions in terms of cost and structural performance.

Kalapodis et al. (2020) compared three performance-based seismic design methods for plane steel braced frames.

Moghaddam et al. (2021) presented a performance-based optimization framework for optimal cross-sectional distribution of steel moment-resisting frames subject to earthquake excitations.

In the present research, the feasibility of nonlinear analysis for the seismic design of RC special moment frames has been investigated. A PBD method for the seismic design of such frames is presented that involves the use of advanced analytical tools. The method then investigated by applying to a regular multi-story RC frame building and the seismic performance of this building is

compared with that of a similar building designed to current seismic code. Figure (1) is a flowchart of the seismic design approach of this research.

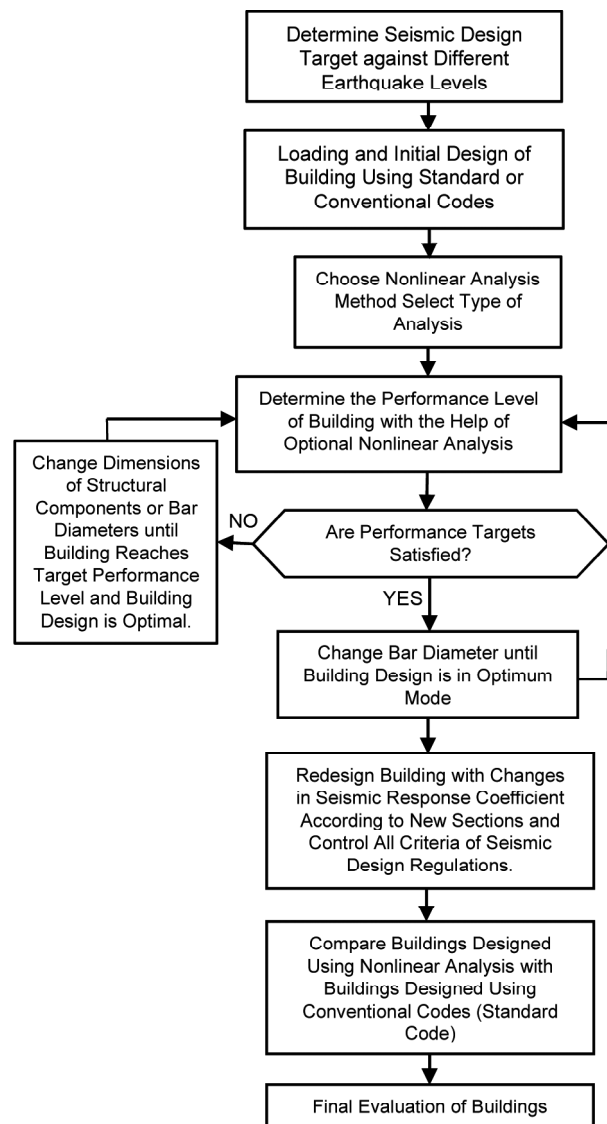


Figure 1. Flowchart of seismic design approach using nonlinear analysis.

2. Determination of Seismic Design Target

The determination of the seismic design objective using nonlinear analysis is essential for the seismic design of buildings. The choice of design objective is influenced by employer requirements and the significance of the building from the historical, economic, social, technical and safety aspects. The use of nonlinear analysis in the seismic design includes the maximum damage allowed for building components (expected performance level) and the seismic hazard level (earthquake shaking).

The objective in BHRC is to protect the building against the effects of earthquake hazard level 1. These are earthquakes with a return period of 475 years (probability of exceedance of 10% in 50 years) for which the objectives can minimize mortality and can satisfy the life-safety (LS) performance level. Hazard level 1 in BHRC is called the design-basis earthquake.

3. Analytical Model and Ground Motions

3.1. Specifications of the Model

The building was designed using linear static analysis in accordance with ACI 318 (2014) code, and the seismic loading and analysis was based on BHRC, which is similar to ASCE/SEI 7-16. The building had a regular 4-story 3D RC special moment frame with a force reduction factor of 7.5 ($R_u = 7.5$). It is assumed as a residential/office building for which the first and second stories were offices and the third and fourth stories were residential. The building was located in Tehran, a city with very high seismicity, on soil type II (V_s (shear-wave velocity) = 375-750 m/sec). The compressive strength and Young's modulus of the RC were 25 MPa and 26 GPa, respectively. The yield strength of the longitudinal and transverse reinforcement steel was 400 and 340 MPa, respectively, with a Young's modulus of 200 GPa. Figure (2) shows the plan and elevation of the building.

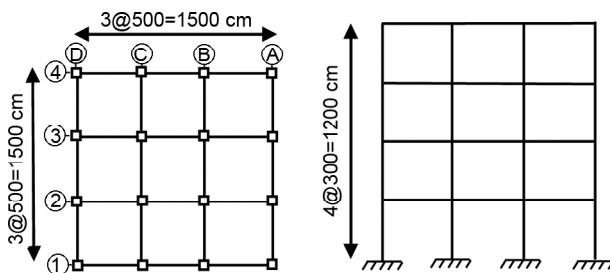


Figure 2. Plan and elevation of four-story modeled building.

The dead load for the typical stories, roof and external walls were 645 kg/m², 575 kg/m² and 610 kg/m, respectively. The live loads of the residential and office stories and the interior partition walls were 200 kg/m², 250 kg/m² and 100 kg/m², respectively. The seismic mass included 100% of the dead load and 20% of the live load.

The dimensions of the beams and columns were defined as multiples of 5 cm. The beams and columns were square in shape and the rebar distribution along the length of the members was uniform. The beam dimensions were selected to be smaller than the column dimensions in order to facilitate reinforcement placement into the beam-to-column connections and improve connection performance, as well as to observe the strong-column and weak-beam criteria. According to US codes, the minimum column dimension is 12 in (300 mm), which is often impractical. A 16-in (400 mm) minimum dimension is suggested, except for unusual cases or for low-rise buildings (Moehle, 2015). The dimensions of the structural components are shown in Table (1). The abbreviation for each building was developed according to the type of analysis used for its design. The first building was designed with linear static analysis (LSA). The second building was designed with nonlinear static analysis (NSA). The third building was designed with nonlinear dynamic analysis (NDA). The modal analysis results of LSA building (LSAB) are shown in Table (2).

3.2. Application of Nonlinear Analysis Methods

The types of analyses used in the framework of PBD are either static (pushover) or dynamic (time-history). In this research, nonlinear static analysis in accordance with appendix 2 of BHRC, which is very similar to ASCE/SEI 41-13 (2013), and nonlinear dynamic analysis, in accordance with

Table 1. Design results of LSA.

Building	Story	Beam		Column			
		b (cm)	h (cm)	b (cm)	h (cm)	Reinforcement	
						Number of Bars	Bar Size
LSAB	1	40	40	45	45	16	16
	2	40	40	45	45	16	16
	3	35	35	40	40	8	16
	4	35	35	40	40	8	16

Table 2. Modal analysis results of LSAB and NSAB.

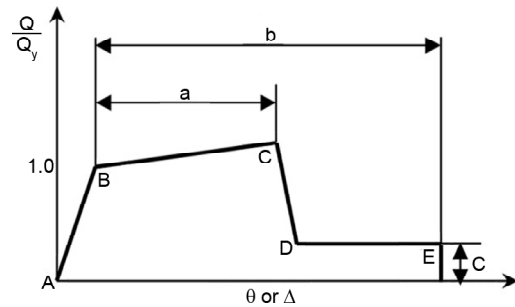
Mode. No	Period (sec)	Modal Participating Mass Ratio	
		X	Y
1	0.84	77.00	0.08
2	0.84	0.08	77.00
3	0.72	0.00	0.00
4	0.27	2.80	12.10
5	0.27	12.10	2.80
6	0.23	0.00	0.00
7	0.13	3.70	1.60
8	0.13	1.60	3.70
9	0.11	0.00	0.00
10	0.08	0.76	1.90
11	0.08	1.90	0.76
12	0.07	0.00	0.00

chapter 16 of the FEMA P-2082-1, was used for the design and evaluation of buildings.

3.3. Nonlinear Modeling of frame Members

The three LSA, NSA and NDA approaches were performed in SAP2000 software version 19.2.1. Modeling of the nonlinear behavior of frame components with concentrated plastic hinges was done according to ASCE/SEI 41-13. To model the nonlinear behavior of a structural member, it was necessary to determine the force-displacement curve of that member based on laboratory evidence or analysis. The ASCE/SEI 41-13 standard allows the use of the force-deformation curve in Figure (3) instead of test results for RC frame components.

The deformations used for the load-deformation relation in Figure (3) were expressed directly using terms such as strain, curvature, rotation, or elongation. Parameters a and b denote those portions of


Figure 3. Generalized force-deformation relation for concrete elements or components (ASCE 2013).

deformation that occur after yield; that is, plastic deformation. Parameter c is the reduced resistance after a sudden reduction from C to D. Parameters a, b and c are defined numerically in the tables in chapter 10 of ASCE/SEI 41-13. To all the beams and columns of the building moment hinges (M) and axial load moment interaction hinges (PMM) are assigned respectively. Plastic hinges are considered at the beginning and end of the beams and columns. The HHT (Hiber-Hughes-Taylor) direct integration method with damping ratio of 5% is used to solve the Differential equations.

3.4. Far-Fault Ground Motion Ensemble

Nonlinear evaluation and redesign of the LSAB were done using NDA. Eleven far-fault ground motions were selected from the FEMA-P695 (2009). All the selected ground motions correspond to NEHRP soil class C. The detailed characteristics of the selected ground motions are given in Table (3). The method of applying far-fault ground motion components to buildings is such that the component with a larger PGA was applied in

Table 3. Characteristics of ground motions used in building design and preliminary evaluation (FEMA-P695).

NO	Year	Identifier	Earthquake	MS	Station	PGA _x (g)	PGA _y (g)	PGV (cm/sec)	Rrup (km)	V _{s_30} (m/sec) ^a
1	1990	ABR	Manjil	7.37	Abbar	0.51	0.50	42.47	12.55	723.95
2	1976	TMZ	Friuli,Italy	6.5	Tolmezzo	0.36	0.31	22.04	15	425.5
3	1992	JOS	Landers	7.28	Joshua Tree	0.28	0.27	43.06	11.03	379.92
4	1999	ARC	Kocaeli	7.51	Arcelik	0.22	0.15	17.69	10.56	523
5	1995	NIS	Kobe	6.9	Nishi Akashi	0.51	0.50	37.29	7.8	609
6	1999	HEC	Hector	7.13	Hector	0.34	0.27	41.74	10.35	726
7	1994	ORR	Northridge	6.69	Castaic Old Ridge RT	0.57	0.51	51.83	20.11	450.28
8	1999	TCU045	Chi-Chi,Taiwan	7.6	TCU045	0.51	0.47	46.38	26	705
9	1999	TCU095	Chi-Chi,Taiwan	7.6	TCU095	0.71	0.39	49.15	13.3	446.63
10	1999	TCU039	Chi-Chi,Taiwan	7.6	TCU039	0.21	0.15	50.02	19.89	540.66
11	1999	TCU070	Chi-Chi,Taiwan	7.6	TCU070	0.26	0.17	52.16	19	401.26

a: NEHRP Site Class = B for VS (Shear-Wave Velocity) = 760–1500 m/s; C for VS = 360–760 m/s; D for VS = 180–360 m/s.

the X direction and the component with a smaller PGA was applied in the Y direction. All ground motions were scaled in accordance with FEMA P-2082-1 and NIST/GCR11-917-15 (2011).

4. Performance level of LSAB

The performance level of the building designed with BHRC for a very-high level hazard zone was investigated to determine if it satisfied the target performance level (LS) for earthquake hazard level 1. The building was subjected to NSA and NDA and its performance level was determined. The target displacement, lateral load patterns, and gravity load patterns were estimated based on the provisions and recommendations in appendix 2 of BHRC. The building was subjected to NSA and NDA under the records listed in Table (3).

The performance level of the LSAB is reported in Table (4), also for each far-fault record is reported separately in Table (5). The building satisfied the LS performance level in all static loading tests. For NDA, the LS performance level was not satisfied for the ORR earthquake (Figure 4). The results of the analysis showed that the design of the primary building (LSAB) was not satisfactory. In order to optimize the primary building in an economical manner to meet the LS performance level, the building was redesigned based on the

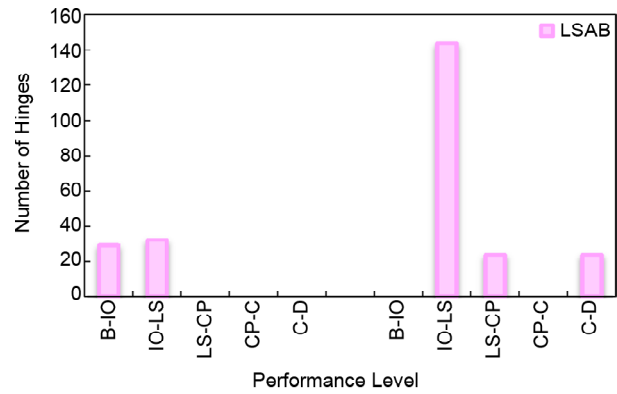


Figure 4. Number of plastic hinges in LSAB under ORR earthquake.

results of nonlinear analysis as explained in the following sections.

5. Description of the Design Procedure Used

The way in which the seismic resistance is distributed in a building affects its seismic behavior. Therefore, instead of focusing on the lateral loading pattern, it is important to focus on the resistance distribution in the building. To satisfy the performance criteria by changing member properties, four methods are applied. They are:

1. Changing the area of the beams while keeping the area of the columns and longitudinal reinforcements constant.
2. Changing the area of the columns and longitudinal reinforcements while keeping the area of the beams constant.
3. Changing the area of the columns, beams and longitudinal reinforcements simultaneously.
4. Changing the area of longitudinal reinforcement while keeping the areas of the beams and columns constant.

When changing the area of the beams while keeping the area of the columns and longitudinal reinforcements constant, in order to achieve an optimal resistance distribution in some stories, the area of the beams were so small that the beams could not satisfy the target LS performance level. Changing the area of the beams, columns and longitudinal reinforcement simultaneously increased the complexity of the problem. Because it is found that the beams play a small role in achieving the appropriate optimal distribution resistance within the target performance level range, therefore, the area of the beams was held constant over the

Table 4. Performance level of LSAB.

Building	Type of Nonlinear Analysis	Performance Level	Target Performance Level
LSAB	NSA	LS	LS
	NDA	D	LS

Table 5. Performance level of LSAB in NDA.

No.	Identifier	Performance Level	Target Performance Level
1	ABR	LS	LS
2	TMZ	LS	LS
3	JOS	LS	LS
4	ARC	IO	LS
5	NIS	LS	LS
6	HFC	LS	LS
7	ORR	D	LS
8	TCU045	LS	LS
9	TCU095	LS	LS
10	TCU039	IO	LS
11	TCU070	LS	LS

Table 6. Design results of NSA.

Building	Story	Beam		Column			
		b (cm)	h (cm)	b (cm)	h (cm)	Reinforcement	
						Number of Bars	Bar Size
NSAB	1	40	40	45	45	8	18
	2	40	40	45	45	8	18
	3	35	35	40	40	8	16
	4	35	35	40	40	8	16

Table 7. Design results of NDA.

Building	Story	Beam		Column			
		b (cm)	h (cm)	b (cm)	h (cm)	Reinforcement	
						Number of Bars	Bar Size
NDAB	1	40	40	50	50	8	20
	2	40	40	50	50	8	20
	3	35	35	45	45	8	18
	4	35	35	45	45	8	18

whole design process, and only the area of the columns and longitudinal reinforcement was changed. The most effective choice was to change the area of the columns and longitudinal reinforcement simultaneously or change only the area of the longitudinal reinforcement.

The building subjected to NDA was also designed using the same method (by changing the longitudinal reinforcement area). After repeated NDA of the building, the design targets were not satisfied when only the longitudinal reinforcement area was changed. For this reason, the areas of the columns and longitudinal reinforcement were changed simultaneously. In the nonlinear dynamic design, ensemble of 11 far-fault records was used as the design earthquake. In the overall design process, all design provisions and RC special moment frame building criteria as the design of the buildings under LSA (Section 3.1) were considered.

The dimensions of the structural components designed with NSA in accordance with appendix 2 of BHRC and NDA in accordance with chapter 16 of FEMA P-2082-1 under the records listed in Table (3) are reported in Tables (6) and (7). The modal analysis results for the two buildings designed using NSA and NDA are reported in Tables (2) and (8), respectively. The second building was designed with NSA (NSAB) and the third building was designed with NDA (NDAB). The areas of the columns and longitudinal bars in all three types of building are shown in Figure (5).

Table 8. Modal analysis results of NDAB.

Mode. No	Priord (sec)	Modal Participating Mass Ratio	
		X	Y
1	0.78	75.7	0.07
2	0.78	0.070	75.7
3	0.67	0.00	0.00
4	0.24	3.2	12.4
5	0.24	12.4	3.2
6	0.21	0.00	0.00
7	0.11	4.1	1.8
8	0.11	1.8	4.1
9	0.10	0.00	0.00
10	0.06	0.74	2
11	0.06	2	0.76
12	0.06	0.00	0.00

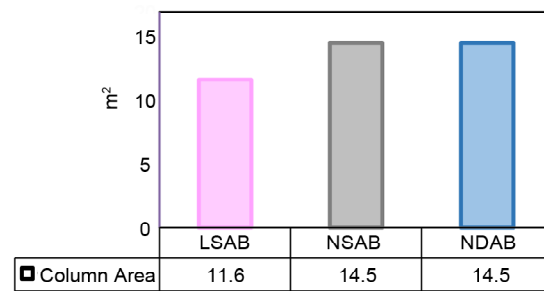
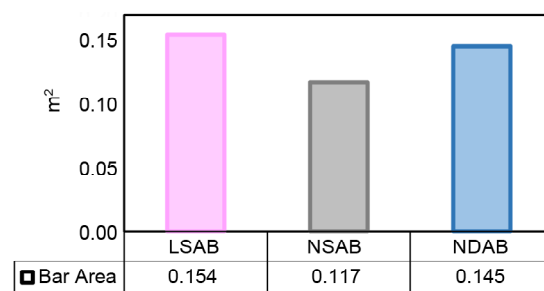


Figure 5. Materials for all designs (LSAB, NSAB and NDAB).

6. Initial Evaluation of Alternative Designs

6.1 Comparisons of Materials

Figure (5) shows that the areas of longitudinal reinforcement obtained in the NDAB and NSAB were smaller than the LSAB, but the amount of concrete used in the NDAB was slightly more than in the LSAB and NSAB. The section dimensions for the NDAB components were large with a small percentage of longitudinal reinforcement. Due to the large cost difference between the concrete and reinforcements, the large sections with low percentages of reinforcement are more economical than smaller sections with a high percentage of reinforcement. In the LSAB, the capacity of many of the members of the building remains unused, which is not economical. In the method used, the capacity of each member with additional capacity will be reduced and each member with a capacity shortage will be given more capacity. Thus, the design of the building will change and the building will be modified and goes towards the optimal building.

6.2. Inter-Story Drift Ratio Demands

Figure (6) compares the average maximum inter-story drift ratios of the LSAB and NDAB in the X and Y directions subjected to NDA under the set of ground motions shown in Table (3). In NDA, in accordance with FEMA P-2082-1, the average story drift ratio for each story should not exceed 1.25 the limits of table 12.12-1 in ASCE/SEI 7-16. This value for buildings with four stories at earthquake hazard level 1 is 0.025 h. The results showed that, in none of the cases were the average story drift ratios in the NDA were greater than the allowed value. Figure (6) shows that the average maximum inter-story drift ratios in all stories of the NDAB in both the X and Y directions were lower than those for the LSAB. On average, the average maximum inter-story drift ratios in the NDAB compared to the LSAB in the X and Y directions decreased 8% and 15%, respectively.

Figure (7) compares the results for NSA of appendix 2 of BHRC for inter-story drift ratios of the LSAB and NSAB. In the NSA, the most critical loading was selected for comparison. In accordance with appendix 2 of BHRC, the maximum inter-story drift ratio for the target

displacement should not be greater than 120% of acceptable values for linear analysis in the code. This value is exactly the same as in ASCE/SEI 7-16. The average story drift ratios in NSA were not greater than the allowed value. Figure (7) shows that the maximum inter-story drift ratios values in the LSAB were very close to the NSAB values. Only the NSAB had, on average, a 5% increase

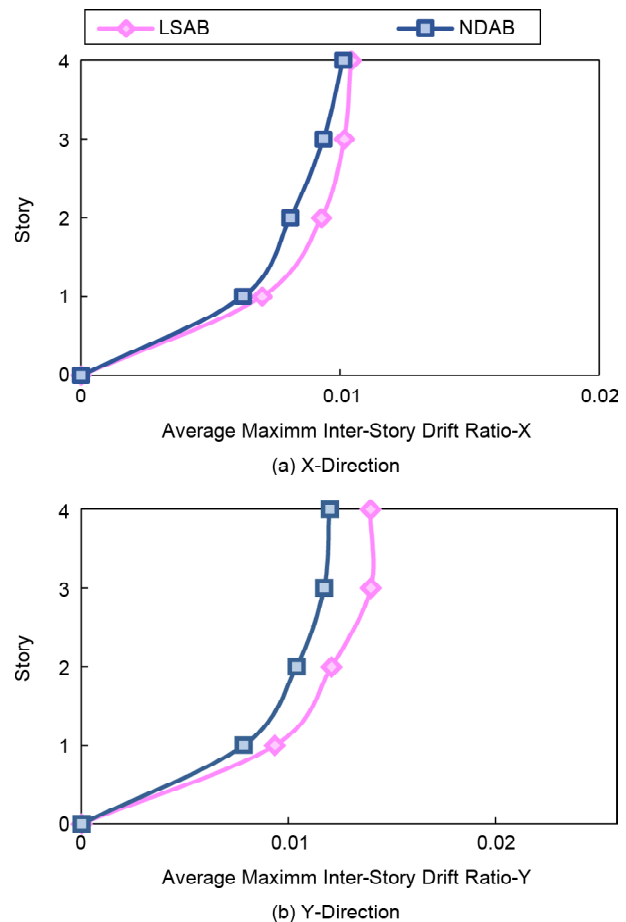


Figure 6. Average maximum inter-story drift ratios of NDA under design and preliminary evaluation of ground motions for LSAB and NDAB.

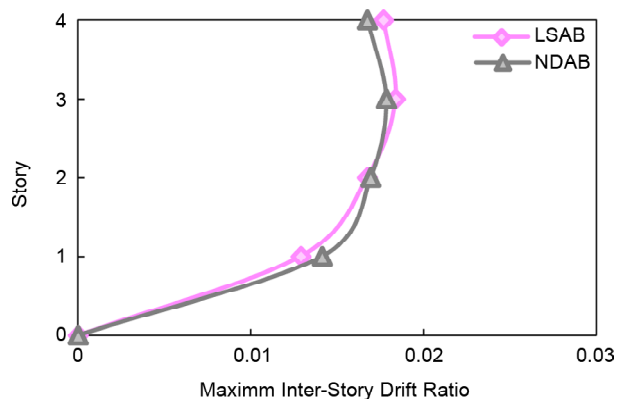


Figure 7. Maximum inter-story drift ratios of NSA in critical load combination for LSAB and NDAB.

in the first and second stories and a 4% decrease in the third and fourth stories.

6.3. Assessment of Seismic Performance

One of the strategies for assessing the efficiency of the method used in the seismic design of the buildings is to compare the performance levels, also the number and locations of the plastic hinges of the LSAB with NSAB and NDAB. The performance levels in the LSAB and NDAB derived from NDA and LSAB and NSAB derived from NSA were compared in Tables (9) and (10), respectively.

Table 9. Performance level for LSAB and NSAB.

Building	Type of Nonlinear Analysis	Performance Level	Target Performance Level
LSAB	NSA	LS	LS
NSAB	NSA	LS	LS

Table 10. Performance level for LSAB and NDAB in NDA.

Earthquake		Performance Level	
NO.	Identifier	LSAB	NDAB
1	ABR	LS	LS
2	TMZ	LS	LS
3	JOS	LS	LS
4	ARC	IO	IO
5	NIS	LS	LS
6	HEC	LS	LS
7	ORR	D	LS
8	TCU045	LS	LS
9	TCU095	LS	LS
10	TCU039	IO	IO
11	TCU070	LS	LS

Figure (8) shows the average number and location of the plastic hinges for eleven records. These figures were derived from the average number of plastic hinges. Figure (9) also shows the number of plastic hinges in NSA for both LSAB and NSAB for the critical load combination. The figures and tables indicate that the NDAB and NSAB satisfied the target performance level (LS). The number of plastic hinges of the NDAB and NSAB was less than those of the LSAB. This indicates that the damage was reduced in the NDAB and NSAB and that most of the plastic hinges in the three types of building were in the beams. Compared to the LSAB, the NDAB and NSAB had

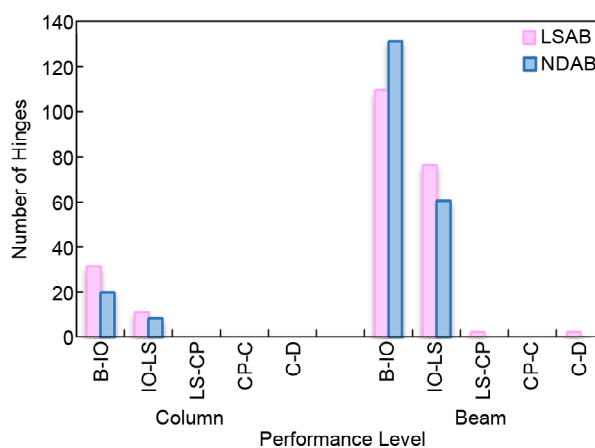


Figure 8. Number of plastic hinges in LSAB and NDAB under design and preliminary evaluation of ground motions.

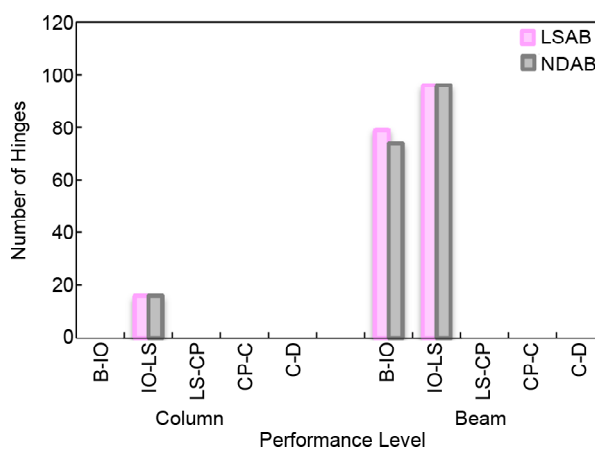


Figure 9. Number of plastic hinges in LSAB and NSAB for critical load combination.

more plastic hinges in the beams and none of the column hinges passed the LS level. This indicates that the strong-column, weak-beam rule was observed in the seismic design of RC special concrete moment frame; thus, the proposed design method was closer to the design objectives.

7. Final Evaluation of Proposed Methodology

The results of NDA (time-history) can be used to investigate the efficiency of proposed method in the seismic design of buildings. All three types of buildings were analyzed under the second set of ground motions with the characteristics and features specified in Table (11). The average maximum inter-story drift ratio demands and seismic performance were compared.

7.1 Far - Fault and Near Fault Ground Motion Ensemble

A total of 22 near-fault and far-fault ground

Table 11. Characteristics of ground motions used in evaluation of buildings.

	NO	Year	Identifier	Earthquake	MS	Station	PGA _x (g)	PGA _y (g)	PGV (cm/sec)	Rrup (km)	Vs ₃₀ (m/sec)	T _p ^b (S)
Far-Fault Ground Motions	1	1971	ORR	San Fernando	6.61	Castaic - Old Ridge Route	0.32	0.27	17.06	22.63	450.28	-
	2	1971	LAK	San Fernando	6.61	Lake Hughes #12	0.38	0.28	16.37	19.3	602.1	-
	3	1989	WAH	Loma Prieta	6.93	WAHO	0.65	0.37	38.12	17.47	388.33	-
	4	1978	DAY	Tabas_Iran	7.35	Dayhook	0.41	0.32	27.12	13.94	471.53	-
	5	1992	MVH	Landers	7.28	Morongo Valley Fire Station	0.22	0.16	29.94	17.36	396.41	-
	6	1980	BRZ	Irpinia_Italy-01	6.9	Bricenza	0.22	0.18	13.10	22.56	561.04	-
	7	1992	FFS	Cape Mendocino	7.01	Ferndale Fire Station	0.38	0.26	89.60	19.32	387.95	-
	8	2007	IZN	Chuetsu-oki_Japan	6.8	Iizuna Imokawa	0.63	0.37	76.90	66.44	591.2	-
	9	1979	HRZ	Montenegro_Yugoslavia	7.1	Herceg Novi - O.S.D. Paviviv	0.26	0.22	13.40	25.55	585.04	-
	10	2010	HVS	Darfield_New Zealand	7	Heathcote Valley Primary School	0.63	0.57	22.71	24.47	422	-
	11	1994	UCL	Northridge-01	6.69	LA - UCLA Grounds	0.47	0.27	22.02	22.49	398.42	-
Near-Fault Ground Motions	12	2009	AGL	L'Aquila_Italy	6.3	L'Aquila - Parking	0.33	0.36	36.35	5.38	717	1.981
	13	1999	TCU102	Chi-Chi_Taiwan	7.62	TCU102	0.30	0.17	91.72	1.49	714.27	9.632
	14	2003	BAM	Bam_Iran	6.6	Bam	0.81	0.63	124.12	1.7	487.4	2.023
	15	1992	PET	Cape Mendocino	7.01	Petrolia	0.59	0.66	88.5	8.18	422.17	2.996
	16	1978	TAB	Tabas	7.35	Tabas	0.86	0.85	123.4	2.05	766.77	6.188
	17	1989	STG	Loma Prieta	6.93	Saratoga - Aloha Ave	0.32	0.51	123.40	8.5	380.89	4.571
	18	1992	SYL	Northridge-01	6.69	Sylmar - Olive View Med FF	0.84	0.60	129.37	5.3	440.54	2.436
	19	1984	GIL	Morgan Hill	6.19	Gilroy Array #6	0.29	0.20	36.50	9.87	663.31	1.232
	20	1999	IRI	Duzce_Turkey	7.14	IRIGM 487	0.28	0.30	38.94	2.65	690	10.05
	21	1979	BSO	Montenegro_Yugoslavia	7.1	Bar-Skupstina Opstine	0.37	0.36	41.24	6.98	462.23	1.442
	22	1999	TCU052	Chi-Chi_Taiwan	7.62	TCU052	0.35	0.45	172.33	0.66	579.1	11.96

b: Velocity pulse period

motions that differed from the design earthquakes were selected from the PEER (1998). Eleven of these records were far-fault and others were near-fault with forward-directivity effects. The records were selected and scaled in accordance with the provisions and recommendations of FEMA P-2082-1. The characteristics of the ensembles used for the final evaluation of the methodology are shown in Table (11). The accelerograms were selected such that they all had the same characteristics (magnitude, fault distance, rupture mechanism, and source mechanisms).

The event magnitude ranged from M6.5 to M7.6 and the site-source distance for far-fault ground motion was greater than 10 km and for near-fault ground motions was less than 10 km. The peak ground acceleration values (PGA_{max}) ranged from 0.21 g to 0.86 g. The far-fault ground motion component with a larger PGA was applied in the X direction and the component with a lower PGA was applied in the Y direction. For the

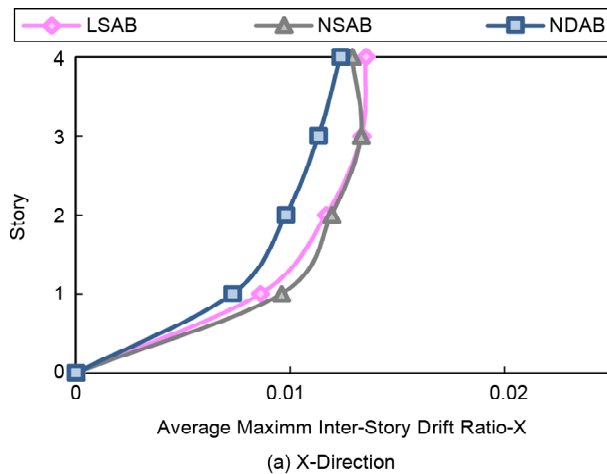
near-fault ground motion, in order to investigate the effects of accelerograms with pulses, the fault-parallel component was applied in the X direction and the fault-normal component was applied in the Y direction.

7.2 Average Maximum Inter-Story Drift Ratio Demand

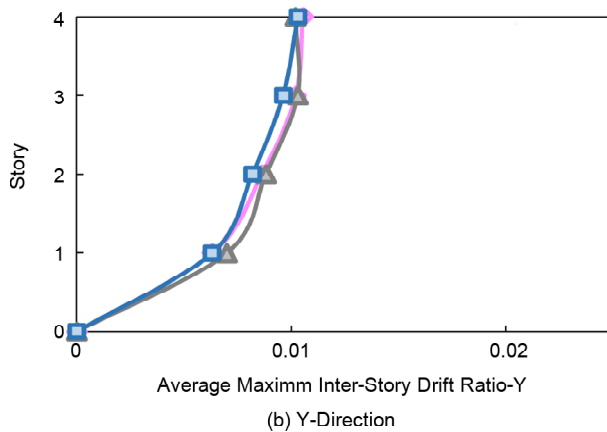
7.2.1 Far-Fault Ground Motions

Figure (10) shows the average maximum inter-story drift ratios for the LSAB, NSAB, and NDAB under the eleven far-fault records in Table (11) in both X and Y directions. It was observed that the average maximum inter-story drift ratios in the NDAB on almost all stories in X and Y directions were lower than that of the LSAB and NSAB.

In the X direction on the first and the second stories, the maximum values were for the NSAB and, on the third and fourth stories, they were for the LSAB. In the Y direction, on the first, the second and the third stories, they were for the NSAB and, on the fourth story, for the LSAB.



(a) X-Direction



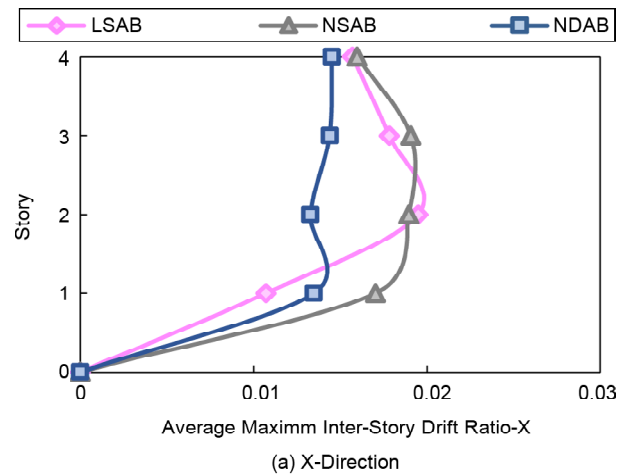
(b) Y-Direction

Figure 10. Average maximum inter-story drift ratios of NDA under far-fault evaluation of ground motions for LSAB, NSAB and NDAB.

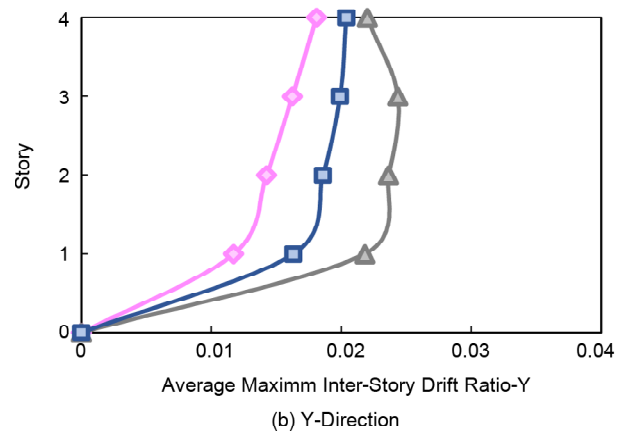
The maximum inter-story drift ratios in the NDAB compared to the LSAB in the X direction decreased an average of 13% and, in the Y direction, decreased an average of 4%. In the NSAB compared to the LSAB in the X direction, on the first and the second stories, they increased an average of 7% and, on the third and the fourth stories, decreased an average of 3%. In the Y direction, on the first, the second and the third stories, they increased an average of 5% and, on the fourth story, decreased an average of 3%. The results presented in this section and those reported in Section 6.2 are in good agreement.

7.2.2. Near-Fault Ground Motions

The results of NDA of buildings under near-fault ground motions for all three types of building designed with LSA according to BHRC, NDA in accordance with appendix 2 of BHRC and NDA in accordance with chapter 16 of the FEMA P-2082-1 were compared. The average maximum



(a) X-Direction



(b) Y-Direction

Figure 11. Average maximum inter-story drift ratios of NDA under near-fault evaluation of ground motions for LSAB, NSAB and NDAB.

inter-story drift ratios are shown in Figure (11). They show the average maximum inter-story drift ratios for the LSAB, NSAB and NDAB under the eleven near-fault records from Table (11) in both X and Y directions.

In the X direction, the first story of the NSAB and the second, the third and the fourth stories of the NDAB recorded the smallest average maximum inter-story drift ratios. The highest values in all stories except the second story were in the NSAB. In the Y direction, all stories of the LSAB had the lowest average maximum inter-story drift ratios compared to the NSAB and NDAB. The NSAB had the largest values in all stories compared to the two other buildings.

The average maximum inter-story drift ratios in the NDAB compared to the LSAB in the X direction on the first story increased an average of 26% and on the second, the third and the fourth stories decreased an average of 20%. In the Y direction, the values for all stories increased

an average of 25%. In the NSAB compared to the LSAB in the X direction, on the first, the third and the fourth stories, they increased an average of 23% and, on the second story, decreased an average of 3%. In the Y direction, the values for all stories increased an average of 56%.

7.3. Final Assessment of the Seismic Performance

7.3.1 Performance Levels, Number of Plastic Hinges in LSAB, NSAB and NDAB.

Tables (12) and (13), respectively, list the performance levels of all three types of building for the far-fault and near-fault ground motions. Figures (12) and (13), respectively, show the average number of plastic hinges for the far-fault and near-fault ground motions. In Tables (12) and (13) for the far-fault earthquakes, the performance level of the NDAB for the ORR, MVH and HVS earthquakes changed from LS to

immediate occupancy (IO), in the IZN earthquake, the performance level changed from collapse prevention (CP) to D. The other far-fault earthquakes and all near-fault earthquakes show identical performance levels for all three types of building.

Figures (12) and (13) show that, for the far-fault and near-fault ground motions, the greatest and least damage occurred for the NSAB and NDAB, respectively. Most of the plastic hinges in all three types of building were in the beams, with the damage for the beams being 80% more than for the columns. The damage in the NDAB compared to the LSAB in regions under far-fault and near-fault ground motions decreased 7% and 4%, respectively. In the NSAB, they increased 1% and 2%, respectively. In the LSAB and NDAB, none of the plastic column hinges exceeded the

Table 12. Performance level for LSAB, NSAB and NDAB under far-fault evaluation of ground motions.

Earthquake		Performance Level		
NO.	Identifier	LSAB	NSAB	NDAB
1	ORR	LS	LS	IO
2	LAK	IO	IO	IO
3	WAH	LS	LS	LS
4	DAY	LS	LS	LS
5	MVH	LS	LS	IO
6	BRZ	IO	IO	IO
7	FFS	D	D	D
8	IZN	CP	CP	D
9	HRZ	IO	IO	IO
10	HVS	LS	LS	IO
11	UCL	LS	LS	LS

Table 13. Comparison of performance level for LSAB, NSAB and NDAB under the near-fault evaluation of ground motions.

Earthquake		Performance Level		
NO.	Identifier	LSAB	NSAB	NDAB
1	AQL	IO	IO	IO
2	TCU102	D	D	D
3	BAM	D	D	D
4	PET	D	D	D
5	TAB	D	D	D
6	STG	LS	LS	LS
7	SYL	D	D	D
8	GIL	IO	IO	IO
9	IRI	IO	IO	IO
10	BSO	LS	LS	LS
11	TCU052	D	D	D

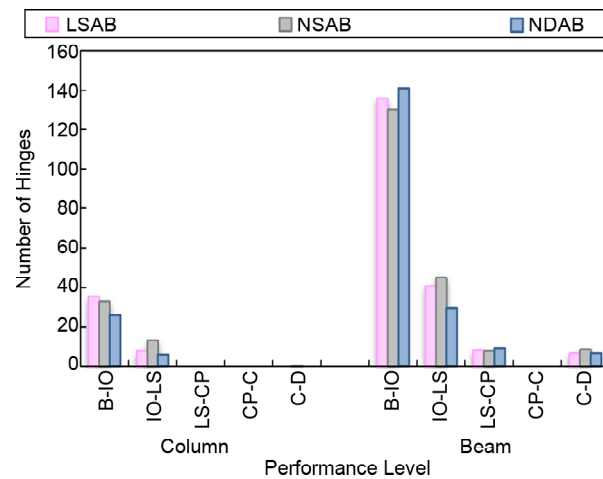


Figure 12. Number of plastic hinges in LSAB, NSAB and NDAB under far-fault ground motions.

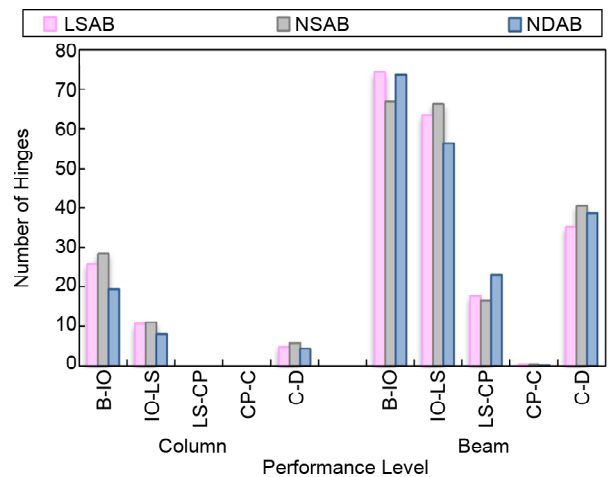


Figure 13. Number of plastic hinges in LSAB, NSAB and NDAB under near-fault ground motions.

LS level; however, in the beams, a number of plastic hinges exceeded the LS level. In the NSAB, few of the column hinges exceeded the LS level. The greatest number of hinges that exceeded the LS level in the columns and the beams were in this type of building. The damage to the columns of the NDAB was 27% lower than of the LSAB. In the NSAB, it was 8% higher than for the LSAB.

In the near-fault earthquakes, beams and columns did not satisfy the LS level, but more hinges in beams than columns exceeded the LS level in the columns of the NSAB than in the LSAB and NDAB. In the NDAB, the number of columns hinges that did not satisfy the LS level was less for the LSAB and NSAB and were mainly in the beams. The damage to the columns of the NDAB was 24% lower than of the LSAB. In the NSAB, it was 10% higher than in the LSAB.

7.3.2. Plastic Hinge Locations

The locations of the plastic hinges for the special moment frames designed using the conventional procedure and the proposed method were compared under near-fault and far-fault ground motions. The comparison was performed using only records that would cause the buildings to exceed the LS level. The results of the spectral accelerations of critical records were compared with the periods of the buildings shown in Figures (14) and (15).

Table (12) shows the results of far-fault records and earthquakes that created a critical state. It reveals that all three types of building exceeded the LS level for FFS and IZN earthquakes. Figure (16a) shows the final plastic hinge locations for special moment frames in the FFS earthquake. For the NDAB, more plastic hinges in the top-story beams exceeded the LS level but, for the LSAB,

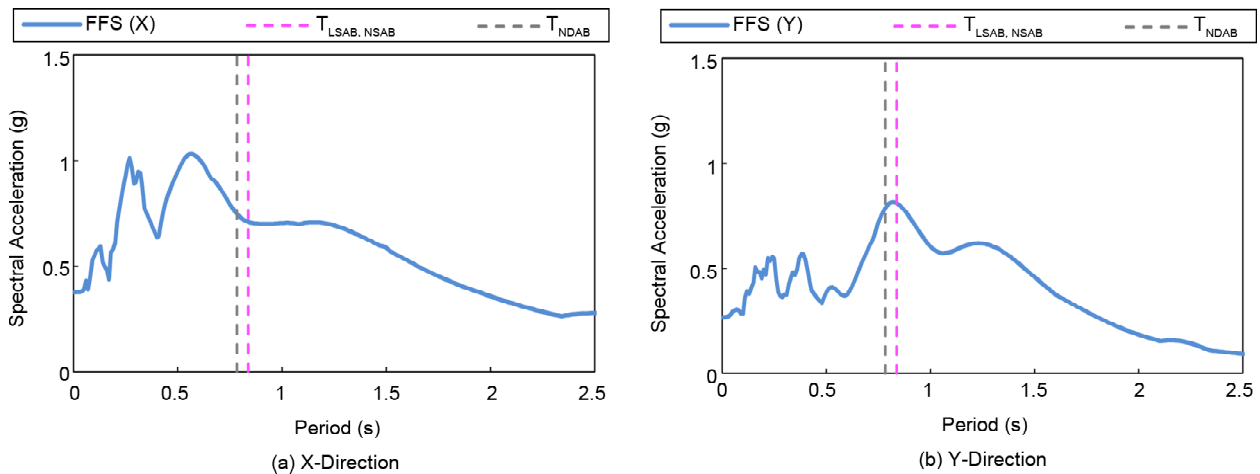


Figure 14. Spectral accelerations of FFS earthquake for periods of LSAB, NSAB and NDAB.

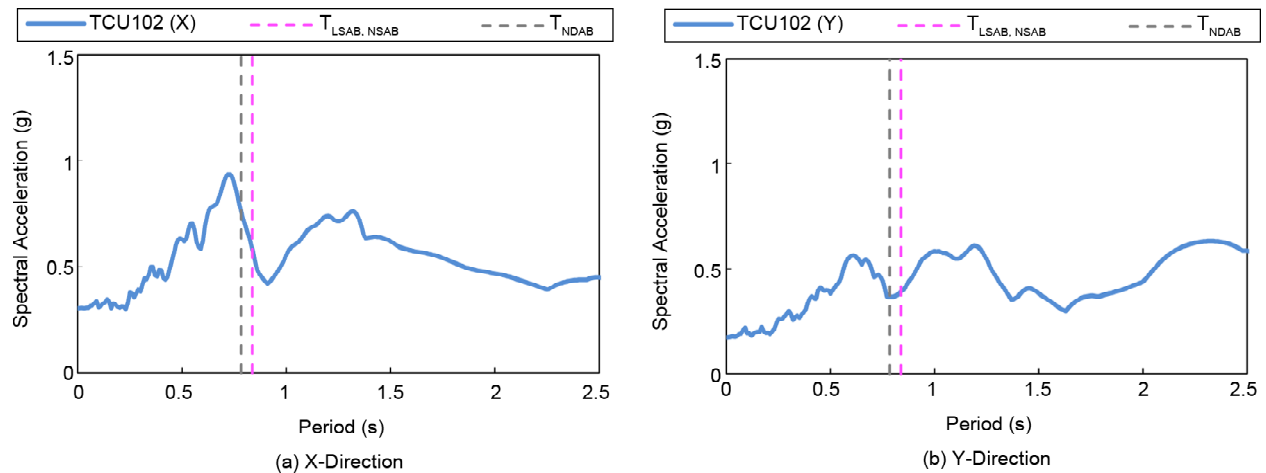


Figure 15. Spectral accelerations of TCU102 earthquake for periods of LSAB, NSAB and NDAB.

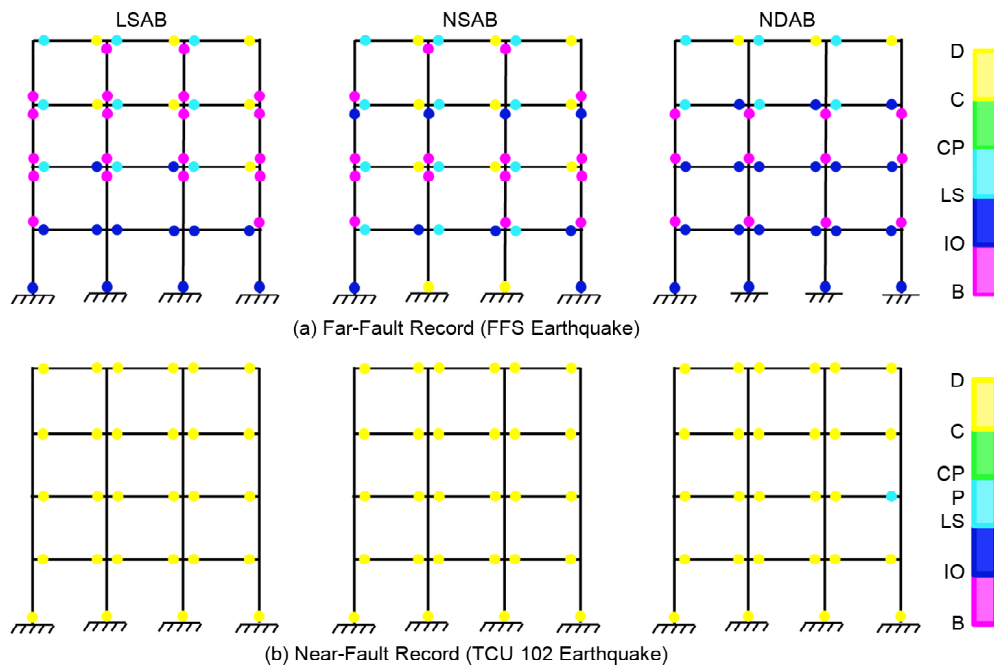


Figure 16. Plastic hinge locations for various design procedures.

this occurred more frequently in the beams in the lower stories. In the NSAB, both the first-story beams and the columns exceeded the LS level. The findings for the IZN earthquake were similar, except that damage occurred on the second story in both the NSAB and LSAB and in the top two stories of the NDAB. The results shown in Sections 7.2.1, 7.3.1 and 7.3.2 reveal the inefficiency of the nonlinear static procedure and the efficiency of the nonlinear dynamic procedure for the design of RC buildings with special moment frames in regions experiencing far-fault ground motion compared with the other types of analyses.

Table (13) shows that, for the near-fault records, the LS level was exceeded in six earthquakes. The TCU 102 earthquake created a critical state. Figure (16b) shows that the plastic hinge locations for the near-fault records in all three types of building were similar, although there was a slight improvement in the NDAB. For example, in the TAB earthquake, the first story columns did not exceed the LS level but those in the LSAB and NSAB exceeded this level. The near-fault record pulses caused plastic hinges to form in all the buildings under excitation at nearly the same moment. Because the earthquake force input in pulse-type records occurred within a short time-frame, the hinges had little opportunity to deform. Thus, to allow the sudden energy to

dissipate, more hinges formed immediately. This caused the formation of plastic hinges at the bottom of the first-story columns, which generally have little capacity for deformation and increased the risk of instability in the building.

The results in Sections 7.2.2, 7.3.1 and 7.3.2 reveal the inefficiency of all three analysis methods in accordance with BHRC, appendix 2 of BHRC and chapter 16 of the FEMA P-2082-1 for the seismic design of RC special moment frames under near-fault ground motions.

8. Conclusions

This study investigates the feasibility of nonlinear analysis for the seismic design of low-rise reinforced concrete special moment frames. One of the innovations of this research is the methodology developed to design building members using nonlinear analysis (static or dynamic). For this purpose, a regular multistory RC frame building was designed using both the proposed and conventional methods. The two methods were first assessed using static and dynamic analyses and the final assessment was also done with dynamic analyses using more ground motions. The results are as follows for the regular multistory frame buildings to which it has been applied:

With the use of nonlinear analysis in the design of moment frames, performance objectives can be

explicitly incorporated into the seismic design. This allows a building for a region with a particular seismicity level to be designed to achieve the expected performance level for its maximum capacity.

It was demonstrated that achieving the optimal resistance distribution using non-linear analysis can differ depending on the type of non-linear analysis and lateral loading. In nonlinear dynamic analysis, the resistance distribution pattern at the target performance level differed according to the type of design earthquake. Different earthquakes lead to buildings with different member dimensions.

When a building was designed using nonlinear analysis for a specific performance level and earthquake, the construction costs and damage rate decreased. The design procedure used for RC special moment frame produced a more economical design for longitudinal reinforcement.

Nonlinear dynamic analysis provided a more appropriate resistance distribution and building that better met the design objectives. Such a building demonstrated the best behavior in the design earthquake and in earthquakes with characteristics similar to design earthquake than the two other buildings done in far-field regions. Earthquakes with characteristics similar to the design earthquake showed results that were similar to those of the design earthquake.

In regions under far-fault ground motions, the nonlinear static procedure based on appendix 2 of BHRC showed low efficiency. Both the linear static procedure based on BHRC and nonlinear dynamic procedure based on FEMA P-2082-1 showed appropriate efficiency. The nonlinear dynamic procedure was the most suitable approach for the seismic design of RC buildings with special moment frames.

In regions under near-fault ground motions, all three design methods (BHRC, appendix 2 of BHRC and chapter 16 of FEMA P-2082-1) for the seismic design of RC buildings with a special moment frame showed low efficiency. The designs done in nonlinear and linear analysis for near-field regions was insufficient and it is necessary to consider other approaches in order to improve their seismic behavior.

References

- ACI 318 (2014). *Building Code Requirements for Structural Concrete and Commentary*. American Concrete Institute, Farmington Hills, MI, USA.
- ASCE/SEI 41-06 (2007). *Seismic Rehabilitation of Existing Buildings*. American Society of Civil Engineers, Virginia, USA.
- ASCE/SEI 41-13 (2013). *Seismic Evaluation and Retrofit of Existing Buildings*. American Society of Civil Engineers, Virginia, USA.
- ASCE/SEI 7-16 (2016). *Minimum Design Loads for Buildings and other Structures*. American Society of Civil Engineers, Virginia, USA.
- ATC 58 (2009). *Guidelines for Seismic Performance Assessment of Buildings*. Applied Technology Council, Redwood City, USA.
- ATC-40 (1996). *Evaluation and Retrofit of Concrete Buildings*. Applied Technology Council; Redwood City, California.
- BHRC *National Code of Practice for Seismic Resistant Design of Buildings (Standard No. 2800, 4th Edition)*. Tehran, Iran.
- Carvalho, G., Bento, R. & Bhatt, C. (2013). Non-linear static and dynamic analyses of reinforced concrete buildings-comparison of different modelling approaches. *Earthq. Struct*, 4(5), 451-470.
- Deierlein, G. G., Reinhorn, A.M. & Willford, M.R. (2010). Nonlinear structural analysis for seismic design. *NEHRP Seismic Design Technical Brief*, 4, 1-36.
- Eurocode (2003). *Design of Structure for Earthquake Resistance-Part 1: General Rules Seismic Actions and Rules for Buildings*. European Committee for Standardization, Brussels, Belgium.
- Fajfar, P. (2018). Analysis in seismic provisions for buildings: past, present and future. In *Recent Advances in Earthquake Engineering in Europe: 16th European Conference on Earthquake Engineering-Thessaloniki 2018*, 1-49. Springer International Publishing.
- FEMA 273 (1997). *NEHRP Guidelines for the*

- Seismic Rehabilitation of Buildings*. Federal Emergency Management Agency, Washington, DC, USA.
- FEMA 440 (2005). *Improvement of Nonlinear Static Seismic Analysis Procedures*. Federal Emergency Management Agency, Washington, D.C, USA.
- FEMA P-2082-1 (2020). *NEHRP Recommended Seismic Provisions for New Buildings and Other Structures*. Federal Emergency Management Agency, Washington, D.C, USA.
- FEMA P440 (2009). *Effects of Strength and Stiffness Degradation on the Seismic Response of Structural Systems*. Federal Emergency Management Agency, Washington, D.C, USA.
- FEMA-P695 (2009). *Quantification of Building Seismic Performance Factors*. Federal Emergency Management Agency, Washington, DC, USA.
- Fintel, M. & Ghosh, S.K. (1982). Explicit inelastic dynamic design procedure for aseismic structures. *Journal Proceedings*, 79(2), 110-118.
- Ganjavi, B. & Ghodrati Amiri, G. (2018). A comparative study of optimum and Iranian seismic design force distributions for steel moment resisting buildings. *Int. J. Optim. Civil. Eng.*, 8(2), 195-208.
- Gkatzogias, K.I. & Kappos, A.J. (2015). Deformation-based seismic design of concrete bridges. *Earthquakes and Structures*, 9(5), 1045-1067.
- IBC (2012). *International Building Code*. International Code Council ICC, Birmingham AL, USA.
- Kalapodis, N.A., Papagiannopoulos, G.A. & Beskos, D.E. (2020). A comparison of three performance-based seismic design methods for plane steel braced frames. *Earthquakes and Structures*, 18(1), 27.
- Kappos, A.J. & Manafpour, A. (2001). Seismic design of R/C buildings with the aid of advanced analytical techniques. *Engineering Structures*, 23(4), 319-332.
- Kappos, A.J. & Panagopoulos, G. (2004). Performance-based seismic design of 3D R/C buildings using inelastic static and dynamic analysis procedures. *ISET Journal of Earthquake Technology*, 41(1), 141-158.
- Kappos, A.J. & Stefanidou, S. (2010). A deformation-based seismic design method for 3D R/C irregular buildings using inelastic dynamic analysis. *Bulletin of Earthquake Engineering*, 8, 875-895.
- Li, S., Yu, B., Gao, M. & Zhai, C. (2019). Optimum seismic design of multi-story buildings for increasing collapse resistant capacity. *Soil Dynamics and Earthquake Engineering*, 116, 495-510.
- Mergos, P.E. (2017). Optimum seismic design of reinforced concrete frames according to Eurocode 8 and fib Model Code 2010. *Earthquake Engineering & Structural Dynamics*, 46(7), 1181-1201.
- Mergos, P.E. (2018). Efficient optimum seismic design of reinforced concrete frames with nonlinear structural analysis procedures. *Structural and Multidisciplinary Optimization*, 58(6), 2565-2581.
- Mergos, P.E. (2020). Minimum cost performance-based seismic design of reinforced concrete frames with pushover and nonlinear response-history analysis. *Structural Concrete*, 21(2), 599-609.
- Moehle, J.P. (2015). *Seismic Design of Reinforced Concrete Buildings*, 814, New York: McGraw-Hill Education.
- Moghaddam, H., Hajirasouliha, I. & Gelekolai, S.M.H. (2021). Performance-based seismic design of moment resisting steel frames: Adaptive optimisation framework and optimum design load pattern. *In Structures*, 33, 1690-1704, Elsevier.
- NIST/GCR11-917-15 (2011). *Selecting and Scaling Earthquake Ground Motions for Performing Response-History Analyses*. National Institute of Standards and Technology Engineering Laboratory Gaithersburg, Maryland, USA.
- Park, K. (2005) *Conceptual Seismic Design of Regular Frames Based on the Concept of Uniform Damage*. Ph.D. Dissertation, Maryland University, USA.
- PEER (1998). *Pacific Earthquake Engineering Research Center*. Berkeley University, California, USA. <http://peer.berkeley.edu/smcat>.
- Rao, K.P., Balaji, K.V.G.D., Raju, S.G., & Rao, S.S.

(2017). Nonlinear pushover analysis for performance based engineering design-A review. *International Journal for Research in Applied Science & Engineering Technology (IJRASET)*, 5.

Romao, X., Costa, A. & Delgado, R. (2002). Non-linear analysis based seismic design. *Proceedings of the 12th European Conference on Earthquake Engineering*, London, UK.

Teran-Gilmore, A., Sanchez-Badillo, A. & Espinosa-Johnson, M. (2010). Performance-based seismic design of reinforced concrete ductile buildings subjected to large energy demands. *Earthquakes and Structures*, 1(1), 69-92.